

Synthesis and structure of bismuth titanate nanopowders prepared by metalorganic decomposition method

W. L. LIU*

School of Physics and Microelectronics, Shandong University, Jinan 250100, People's Republic of China;
National Laboratory of Crystal Materials, Shandong University, Jinan 250100, People's Republic of China;
Department of Materials Science and Engineering, Shandong Institute of Light Industry, Jinan 250100,
People's Republic of China
E-mail: wlliu@sdu.edu.cn; liuwl@sdli.edu.cn

H. R. XIA

School of Physics and Microelectronics, Shandong University, Jinan 250100, People's Republic of China;
National Laboratory of Crystal Materials, Shandong University, Jinan 250100, People's Republic of China

H. HAN, X. Q. WANG

National Laboratory of Crystal Materials, Shandong University, Jinan 250100, People's Republic of China

Bismuth titanate ($\text{Bi}_4\text{Ti}_3\text{O}_{12}$ (BTO)) belongs to the family of ferroelectric materials with layered structures, which can be written as a general formula of $(\text{Bi}_2\text{O}_2)^{2+}(\text{Bi}_2\text{Ti}_3\text{O}_{10})^{2-}$. The layered structure is constructed by alternative stacking of a triple layer of TiO_6 octahedra (perovskite slab) and a monolayer of $(\text{Bi}_2\text{O}_2)^{2+}$ along the *c*-axis. Single crystal BTO has low dielectric permittivity and a very high Curie temperature ($T_c = 675^\circ\text{C}$), which makes it useful for various applications such as memory elements, optical displays, and piezoelectric converters of pyroelectric devices in a wide temperature range from 20 to 600°C . Above T_c , BTO possesses a paraelectric tetragonal $I4/mmm$ structure proposed by Aurivillius [1]. Below T_c , the structure becomes an orthorhombic $Fmmm$ symmetry, which exhibits ferroelectric properties [2].

BTO ceramics have been used in capacitors, transducers, sensors, etc. [3, 4]. The tuning of electric properties by compositional modification as well as the size effect can meet commercial specifications for Curie temperature, conductivity, coercivity, compliance, etc. [5, 6].

Although BTO is normally prepared by solid-state reaction of Bi_2O_3 and TiO_2 at elevated temperatures up to 1100°C [7], owing to some inherent limitations of this process that yields large grain size of product phase, several alternate chemical syntheses routes have been proposed. These include coprecipitation, sol-gel, hydrothermal and molten salt synthesis [8–11]. Metalorganic decomposition (MOD) employed in this study offers the advantages of low calcining temperature, simplifying process, better homogeneity, stoichiometric composition control, and low cost.

In the experiment, the required amount of bismuth nitrate [$\text{Bi}(\text{NO}_3)_3 \cdot 5\text{H}_2\text{O}$] was added in glacial acetic acid (CH_3COOH) by stirring at 60°C till it is completely dissolved. Stoichiometric tetrabutyl titanate ($\text{Ti}(\text{C}_4\text{H}_9\text{O})_4$) was slowly dropped into the above solution under con-

stant stirring. The acetylacetone ($\text{CH}_3\text{COCH}_2\text{COCH}_3$) as reagent was used to stabilize tetrabutyl titanate. And the solution was diluted with 2-methoxyethanol ($\text{CH}_3\text{OCH}_2\text{CH}_2\text{OH}$) to adjust viscosity and surface tension. The resultant solution was stirred at room temperature for 1 hr and filtered thereafter to form the stock solution, which was yellow, clear, and transparent.

The precursor solution thus obtained was dried in an oven at 90°C for 10 hrs, resulting in the formation of a fine yellowish powder. Thermal reactions taking place during the calcinations of the powder were analyzed in air by thermo-gravimetric and differential thermal analysis (TG/DTA, Netzsch STA 449c). The existing phases in the calcined samples were studied by X-ray diffraction (XRD, Rigaku D/MAX- γ A). Crystallite size of calcined powder was determined by X-ray line broadening using the Scherrer equation [12]. The evolution of the powder morphology with the calcination temperature was studied by a transmission electron microscope (TEM, Hitachi H-800). The Raman measurements were performed in the backscattering geometry using a Ventuno21 NRS-1000DT instrument at room temperature to study the lattice dynamics and structural variety.

The relative weight loss (44%) and differential thermal analysis of the pre-heated precursor, as shown in Fig. 1, indicate that heat begins to evolve at about 300°C and the second weight loss occurs around 600°C . It is seen from the curve of the DTA in this figure that two exothermic effects appear at about 350 and 750°C , respectively. Combined with TGA data, it is obvious that the endothermic effect at about 350°C is due to the decomposition and decarbonization of organic and inorganic compounds. It also demonstrates that the weight loss takes place in the endothermic processing between 270 and 420°C , which is about 24%. The DTA curve shows the exothermic effect at about 350°C , which probably also corresponds to the first

*Author to whom all correspondence should be addressed.

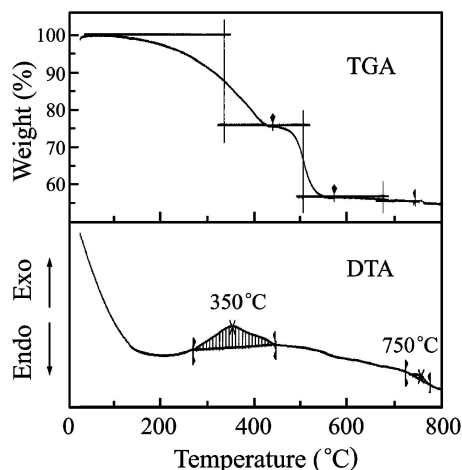


Figure 1 TG/DTA curves for stock precursors.

nucleation events and the solid-state reaction, and it will be discussed in XRD data. With an increase in temperature, the second exothermic effect, which appears to be located at $\sim 750^\circ\text{C}$ is also present. Although no previous thermodynamic data have been found in the literature, the second exothermic effect may be attributed to the formation of small agglomerate of pure BTO ceramic powders, and the crystallization process of BTO is completed before 750°C . At that temperature there is no weight loss. This crystallization process takes place simultaneously with the combustion of residual organic products and/or carbon.

The X-ray diffraction studies on the samples calcined at different temperatures for 5 min are shown in Fig. 2. The XRD pattern of initial powder confirms the amorphous nature, indicating that the powder is non-crystalline. The precursor shows evident crystallization as the temperature increases to 450°C , and the three strong peaks correspond to $\text{Bi}_{12}\text{TiO}_{20}$ and $\text{Bi}_4\text{Ti}_3\text{O}_{12}$, as marked in the figure, respectively. In the short temperature interval of $450\text{--}550^\circ\text{C}$ the precursor converts completely into the bismuth titanate compound (BTO and $\text{Bi}_{12}\text{TiO}_{20}$). Between 550 and 750°C all the amor-

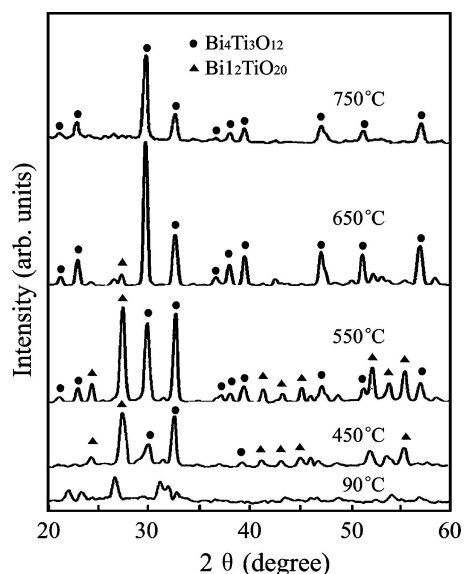


Figure 2 X-ray diffraction patterns of BTO precursor calcined at various temperatures.

phous phases react rapidly with the $\text{Bi}_{12}\text{TiO}_{20}$ intermediate phase leading to the formation of the BTO compound. It is also found from the XRD spectra that BTO powder has orthorhombic phase structure when the annealing temperature is 750°C . The crystallite size of the powder heated at 750°C for 5 min is determined to be ~ 40 nm from the half-width of the X-ray diffraction peaks using Scherrer's equation. An increase in the grain size of BTO powder is observed as the annealing temperature increased up to 650°C but decrease remarkably thereafter. The measured lattice parameters, $a = 0.5449$, $b = 0.5453$, and $c = 3.281$ nm, are slightly different from the orthorhombic single crystal BTO previously reported, which may be due to the lattice distortion in BTO as discussed later in Raman study [2].

Fig. 3 shows the TEM micrographs of bismuth titanate nanoparticles at different calcining temperatures.

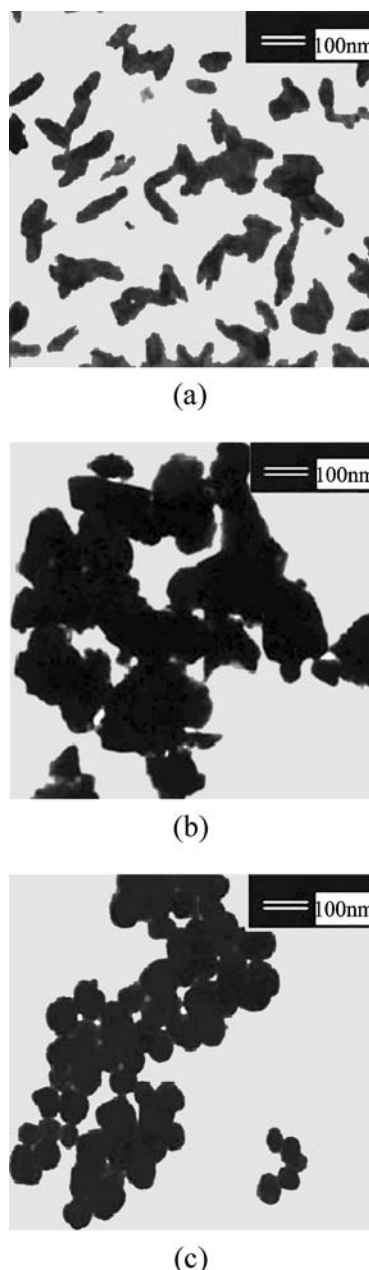


Figure 3 TEM micrographs of initial powder (a), nanocrystalline BTO calcined at 650°C (b), and 750°C (c) for 5 min.

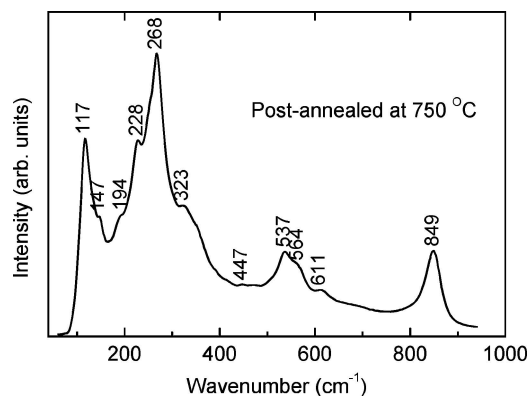


Figure 4 Raman spectra of BTO nanopowders calcined at 750 °C for 5 min.

After drying at 90 °C for 10 hrs, the precursor exhibits rod-like fine grains of about 30 nm in width and 100 nm in length with a narrow size distribution. The average sizes of grains are between 30 and 200 nm after calcining at 650 °C, but the formation of small agglomerates can also be observed. After calcining at 750 °C, the grain sizes reduce to 30–60 nm with a spherical shape. The TEM observations are coincident with the XRD results, and indicate that the BTO nanopowders synthesized by MOD technique have a strong resistance to grain growth and a high thermal stability.

The slight difference on the lattice parameters between the bulk and nanocrystalline BTO may be attributed to the structural distortion. The structural distortion of the material may result in different symmetries. Raman spectra from such regions should reveal the possible symmetry of the material.

Our Raman data on the BTO powder in Fig. 3 agreed with the published results [13]. In accordance with Raman data of $\text{Bi}_4\text{Ti}_3\text{O}_{12}$, BaTiO_3 , and PbTiO_3 [13–15], a shorter bond length of Ti–O than that of Bi–O, suggests that the Raman phonon modes of the corresponding higher wavenumbers, such as the modes at 611 and 849 cm^{-1} , originated mainly from the vibrations of atoms inside the TiO_6 octahedra. The peak at 849 cm^{-1} is attributed to the symmetric Ti–O stretching vibration, while at 611 cm^{-1} to the asymmetric one; the 268 and 228 cm^{-1} modes are ascribed to the O–Ti–O bending vibration. Although the mode at 228 cm^{-1} is Raman inactive according to the O_h symmetry of TiO_6 , it is often observed because of the distortion of octahedron. The mode at 323 is from a combination of the stretching and bending vibrations. The two modes at 537 and 564 correspond to the opposing excursions of the external apical oxygen atoms of the TiO_6 octahedra. The TiO_6 octahedra show considerable distortion at room temperature so that some phonon modes e.g., at 323, 537, 611, and 849 cm^{-1} , appear wide and weak, which are expected to induce ferroelectric anomaly of BTO. The Raman modes of the corresponding lower wavenumbers, such as the modes at 117 cm^{-1} , originated mainly from the vibrations between Bi and O atoms, which can be confirmed by the shift to higher wavenumber due to the modification of a lighter Sm atom at a Bi site with increasing doping concentration [16, 17]. The presence of any additional symmetry that may have originated

from the structural distortions cannot be established. Further study is necessary to clarify the microstructure change due to the size effect of the nanoscaled BTO powder.

In summary, homogeneous and fine BTO ceramic powders have been prepared by metalorganic decomposition method. The synthesis temperatures employed are substantially lower than those currently used in the conventional route. Based on TGA/DTA, and XRD results, we conclude that the synthesis of the BTO compound takes place through the formation of an intermediate phase of composition $\text{Bi}_{12}\text{TiO}_{20}$, which is formed during the heating between 350 and 550 °C. Prolonged heat treatment between 550 and 750 °C promotes a rapid consumption by solid-state reaction of the intermediate phase with the formation of BTO, without any indication on the formation of other different phases or segregation of the individual metal oxides. These results support the contention for the metalorganic precursor synthesis method as useful to prepare ceramics with complex composition such as those of bismuth titanates. The ferroelectricity improvement is expected due to the structural variety as shown in Raman study.

Acknowledgments

The authors thank Dr. Tim Williams (Jasco International Co. Ltd) for technical help. This work was supported by the National Natural Science Foundation of China (10274043), Shandong Provincial Natural Science Foundation and Project for Key Task.

References

1. B. AURIVILLIUS, *Ark. Kemi* **1** (1949) 499.
2. J. F. DORRIAN, R. E. NEWNHAM and D. K. SMITH, *Ferroelectrics* **3** (1971) 27.
3. T. TAKENAKA and K. SAKATA, *J. Appl. Phys.* **55** (1984) 1092.
4. A. FOUSKOVA and L. E. CROSS, *ibid.* **41** (1970) 2834.
5. O. ALVAREZ-FREGOSO, *ibid.* **81** (1997) 1378.
6. T. TAKENAKA and K. SAKATA, *Ferroelectrics* **38** (1981) 769.
7. Y. YONEDA and J. MIZUKI, *Appl. Phys. Lett.* **83** (2003) 275.
8. A. Q. JIANG, G. H. LI and L. D. ZHANG, *J. Appl. Phys.* **83** (1998) 4878.
9. H. S. GU, A. X. KUANG and X. J. LI, *Ferroelectrics* **211** (1998) 271.
10. Q. YANG, Y. LI, Q. YIN, P. WANG and Y.-B. CHENG, *J. Euro. Ceram. Soc.* **23** (2003) 161.
11. T. KIMURA and T. YAMAGUCHI, *Ceram. Int.* **9** (1983) 13.
12. K. P. KLUG and L. E. ALEXANDER, "X-ray Diffraction Procedures" (John Wiley & Sons, New York, 1974).
13. H. IDINK, V. SRIKANTH, W. B. WHITE and E. C. SUBBARAO, *J. Appl. Phys.* **76** (1994) 1819.
14. P. R. GRAVES, G. HUA, S. MYHRA and J. G. THOMPSON, *J. Solid State Chem.* **114** (1995) 112.
15. P. S. DOBAL and R. S. KATIYAR, *J. Raman Spectrosc.* **33** (2002) 405.
16. W. L. LIU, H. R. XIA, H. HAN and X. Q. WANG, *J. Crystal Growth* **264** (2004) 351.
17. *Idem.*, *J. Solid State Chem.*

Received 15 March

and accepted 26 August 2004